A study on the effects of temperature and substrate structure on the templated two-phase film growth via a hybrid model

Xiao Lu, Jia Li, Jian-Gang Zhu, David E. Laughlin, and Jingxi Zhu

Citation: Journal of Applied Physics **123**, 214301 (2018); doi: 10.1063/1.5020871
View online: https://doi.org/10.1063/1.5020871
View Table of Contents: http://aip.scitation.org/toc/jap/123/21
Published by the American Institute of Physics

A study on the effects of temperature and substrate structure on the templated two-phase film growth via a hybrid model

Xiao Lu,[1,2] Jia Li,[1] Jian-Gang Zhu,[2,3] David E. Laughlin,[3,4] and Jingxi Zhu[1,a)]
[1]*Sun Yat-sen University–Carnegie Mellon University Joint Institute of Engineering, School of Electronics and Information Technology, Sun Yat-sen University, Guangzhou, China*
[2]*Department of Electrical and Computer Engineering, Carnegie Mellon University, Pittsburgh, Pennsylvania 15213, USA*
[3]*Data Storage Systems Center, Carnegie Mellon University, Pittsburgh, Pennsylvania 15213, USA*
[4]*ALCOA Professor of Physical Metallurgy, Department of Materials Science and Engineering, Carnegie Mellon University, Pittsburgh, Pennsylvania 15213, USA*

(Received 28 December 2017; accepted 12 May 2018; published online 31 May 2018)

Templated growth of two-phase thin films can achieve desirably ordered microstructures. In such cases, the microstructure of the growing films follows the topography of the template. By combining the Potts model Monte Carlo simulation and the "level set" method, an attempt was previously made to understand the physical mechanism behind the templated growth process. In the current work, this model is further used to study the effect of two parameters within the templated growth scenario, namely, the temperature and the geometric features of the template. The microstructure of the thin film grown with different lattice temperatures and domes is analyzed. It is found that within a moderate temperature range, the effect of geometric features took control of the ordering of the microstructure by its influence on the surface energy gradient. Interestingly, within this temperature range, as the temperature is increased, an ordered microstructure forms on a template without the optimal geometric features, which seems to be a result of competition between the kinetics and the thermodynamics during deposition. However, when the temperature was either above or below this temperature range, the template provided no guide to the whole deposition so that no ordered microstructure formed. *Published by AIP Publishing.*
https://doi.org/10.1063/1.5020871

I. INTRODUCTION

Templated growth of a two-phase thin film, commonly with one phase being crystalline and the other being amorphous, has been successfully demonstrated as a promising technique to control and manipulate the film microstructure at the nanometer scale. With a template composed of a certain pattern which can be prefabricated utilizing the self-assembling block copolymer for pattern transfer[1] or via the nanoimprint technique,[2] the film growth can be guided by template topography. A desirable microstructure from templated growth is obtained with the crystalline phase forming grains on top of geometric features and the amorphous phase filling the grain boundaries, separating the neighboring grains. Such successfully guided templated film growth has been shown to produce desirable film microstructures and to greatly improve the mechanical,[3] thermal,[4] or magnetic[5] properties of the films. Particularly, in the fabrication of magnetic recording media films, the templated growth technique made an even tighter control on the film microstructure than is currently able to be achieved in the industry and thus pushed the limit of the recording capacity. If the grains are periodically grown on geometric features of the template, the grain size, the grain size distribution, and the grain boundary segregant thickness and its distribution in the recording media can be strictly controlled. This opened the door for a reduction in media noise and thus a further increase in the areal density or recording capacity of the current generation media, i.e., CoCrPt-SiO_2-based materials.[6,7]

Furthermore, the fabrication of the FePt+C media film for heat assisted magnetic recording (HAMR), a potential next generation recording technology, requires deposition at elevated temperatures. Therefore, considering the success which the templated growth technique had with the room temperature deposition of the current CoCrPt-SiO_2-based media films, it is of interest to explore the possibility of applying this technique to the high temperature fabrication process of HAMR media.[8] The elevated temperature, in the form of thermal energy, could affect the diffusional behavior of component materials. Different types of diffusion can be activated as substrate temperature varies, and the resultant microstructure could be classified into different zones based on its topography in a structural zone model (SZM).[9–11] However, as templated growth emerged as a new deposition technique in recent years, the SZMs established so far could not fully describe all the mechanisms within the complicated two-phase templated growth in which temperature, substrate topography, composition, *etc.*, are variables.

In a previous study,[12] as a complement to the experimental trials of the templated growth technique,[13] we developed a hybrid computer simulation model to examine how one of the variables, i.e., the topography of the domes on the prefabricated templates, affected the resultant film microstructure. This enabled us to first obtain some understanding

a)Email: zhjingxi@mail.sysu.edu.cn

into the physical mechanisms behind such templated growth. We showed that the main driving force for the simultaneous phase separation during film growth was greatly enhanced by a non-flat topography of the domes on the template, such that at the very initial stage of the film growth, the surface energy gradient dominated the surface diffusion of the mobile species, i.e., SiO_2. It was found in our simulations that templates with the optimized cone-shaped domes [those whose aspect ratio (AR) was greater than the critical value of 0.6] would be required for successful templated growth. Domes of smaller ARs would result in incomplete phase separation.

In the current study, we use the previously developed hybrid model to understand the templated growth process which takes place at elevated temperatures. In particular, we want to understand how thermal effects (such as thermal fluctuations) interplay with the geometric parameters of the template and whether and how the dominant mechanism would change with temperature. With the understanding obtained from this study, we want to initiate some preliminary discussion on applying the templated growth technique to the fabrication of the HAMR media film.

II. METHODOLOGY

The templated growth process involves not only the microstructural evolution at the nanoscale but also the topographic evolution of the film surface at the microscale. The above-mentioned hybrid model, used in this study, realized such multi-scale simulation by coupling the Level set method (LSM),[14,15] and the Potts model Monte Carlo (MC)[16–19] within a three-dimensional discretized space. The LSM part of the model geometrically described how the film surface structure changed as the film grew, while the MC part simulated the diffusion and reorientation of the component materials.

In more detail, for the LSM part, each voxel was assigned a level set value ϕ, and the film surface being deposited was represented by the voxels with ϕ being 0. With a predefined deposition rate $V(\vec{x})$ (set to be constant in this study), the ϕ value of each voxel changed based on Eq. (1), and the zero-ϕ surface could be achieved as time evolves. Thus, the evolution of the film surface being deposited can be tracked by mathematically tracking the surface composed of zero-ϕ at a given simulation step. Initially, the zero-level set surface was set to be the layer that covered the domes on the substrate

$$\frac{\partial \phi}{\partial t} + V(\vec{x}) \cdot \nabla \phi = 0. \tag{1}$$

The film surface or the voxels with $\phi = 0$ were then activated. Materials were added to the zero-level set voxels being activated, while each voxel had a probability of 25% to be occupied by SiO_2 and a probability of 75% to be occupied by CoPt. The out-of-plane orientation of each CoPt voxel was initialized as (0001) to represent the (0001) texture. For the in-plane orientation, a misorientation angle $\theta = 3.6^\circ \times$ k was assigned to each voxel, with k being a random positive integer that was smaller than 101 (360° was equally divided into 100 partitions). Then, the MC simulation was performed on the materials being deposited and the voxels in the layer below the surface. In other words, the MC process was conducted within the top two layers to allow for the inter-layer diffusion effect. The microstructure evolves towards energy minimization with the system Hamiltonian shown in the following equation:

$$H = \frac{1}{2}\left[\gamma_{seg/MM} \cdot \sum_{i=1}^{N_{seg}} \sum_{j=1}^{NN} \left(1 - \delta_{Q_i Q_j}\right) + \gamma_{GB} \cdot \sum_{i=1}^{N_{MM}} \sum_{j=1}^{NN} \left(1 - \delta_{G_i G_j}\right) + \gamma_{MM/sub} \cdot \sum_{i=1}^{N_{sub}} \sum_{j=1}^{NN} \left(1 - \delta_{U_i U_j}\right) + \sum_{i=1}^{N^S} E_i^s\right]. \tag{2}$$

N_{seg}, N_{MM}, and N_{sub} are the number of voxels occupied by the segregant material, by the magnetic material, and by the substrate material, respectively. Integers NN and N^S represent the number of nearest neighbors and the total number of voxels on the surface ($NN = 26$, N^S is dependent on the film morphology). Integers Q_i or Q_j denote whether the site i or j is occupied by segregant (Q_i or $Q_j = 1$) or not (Q_i or $Q_j = 0$). Integer G_i or G_j represents the orientation of the magnetic materials on sites i and j [G_i or $G_j \in (1, 100)$]. Integer U_i or U_j denotes whether site i or j is occupied by a substrate material (U_i or $U_j = 1$) or not. The energy terms are included as follows: $\gamma_{seg/MM}$ is the energy of the segregant/magnetic grain interface, γ_{GB} is the isotropic grain boundary energy of the magnetic material, $\gamma_{MM/sub}$ is the energy of the magnetic material/substrate interface, and E_i^s is the surface energy of material i, proportional to the local curvature following the Mullin theory of surface energy.[20]

During the MC simulations of the deposited layers, the total energy of the film was minimized through the two microevents that were possible to occur to each voxel: diffusion and reorientation of crystalline materials. The probability of each microevent was determined using the following equation:

$$\mathrm{P} = \begin{cases} \dfrac{M}{M_{\max}} \cdot \exp\left(-\dfrac{\Delta E}{k_B T}\right), & \text{if } \Delta E \le 0 \\ \dfrac{M}{M_{\max}}, & \text{otherwise,} \end{cases} \tag{3}$$

where ΔE is the energy change, T is the lattice temperature, and $k_B T$ stands for the thermal fluctuation within the system; M is essentially related to the "rate" at which each event occurs: M stands for atomic mobility during diffusion; for the reorientation, M stands for the rate of the reorientation, similar to the grain boundary migration rate.[21] M was determined using the transition state theory,[22,23] and more details can be found in Ref. 12. The upper bound for probability P was determined as $\frac{M}{M_{\max}}$, and when $\frac{M}{M_{\max}} = 1$, the upper bound becomes 1. Then, the probability of each event was compared to a randomly generated probability P_{rand}. If $P > P_{\mathrm{rand}}$, the microevent is accepted, and otherwise, it is rejected.

Energetic terms are crucial model parameters in a Monte Carlo simulation study. However, to author's best knowledge, there is no extensively quantitative study on interfaces such as SiO_2/CoPt or CoPt/Ru. In this model, we therefore determined $\gamma_{seg/MM}$, γ_{GB}, $\gamma_{MM/sub}$, and E_i^s (two values for two components: i = CoPt and SiO_2) through comparing and matching the simulation result to the experimental result in Ref. 13 at the experimentally optimal condition. Specifically, each energetic parameter was determined by being swept within a range while fixing the other four terms. The details of this determination process and the effect from each parameter are discussed in detail in the Appendix, and a final relation is established as follows: $\gamma_{MM/sub} : \gamma_{GB} : \gamma_{seg/MM} : E^s_{SiO_2} : E^s_{CoPt} = 1 : 5 : 11 : 15 : 21$ (the surface energy of CoPt and SiO_2 was referred from Refs. 24 and 25).

After n number of simulation steps, the current surface was considered to be fully relaxed with the total energy being reduced to a constant level based on the determined energy terms. After testing with different n values, $n = 20000$ was chosen to represent a realistic ratio between the deposition rate and the equilibration rate.[26] The surface of the film with $\phi = 0$ is then renewed by the LSM, and the renewed zero-ϕ surface would undergo a similar MC process to achieve equilibration. Thus, the deposition of the film was simulated by a series of mini-MC processes during which the part of the film being deposited, as determined through LSM, was equilibrated.

This model adopts a simulation box with a lateral size of 200×200, while the z dimension was selected so that the surface of the deposited film was nearly flat. Each voxel represents a 0.5^3 nm^3 space. The size of the system and the voxel were selected to avoid the finite-size effect and the discretization effect and also to be computationally efficient. In Fig. 1, the initial, intermediate, and final stages of a simulated growth on a Ru(002) substrate with predefined domes are shown. In the graph, grey and red colors represent Ru, green blue and orange color represent CoPt, and SiO_2 was colored by black which could maximize the contrast between different materials. The color code of the inverse pole figure was not applied considering the difficulty to efficiently present two types of crystalline materials, CoPt and Ru, and one amorphous SiO_2. In the initial stage, a thin layer of the CoPt+ SiO_2 material was added to the predefined Ru domes,

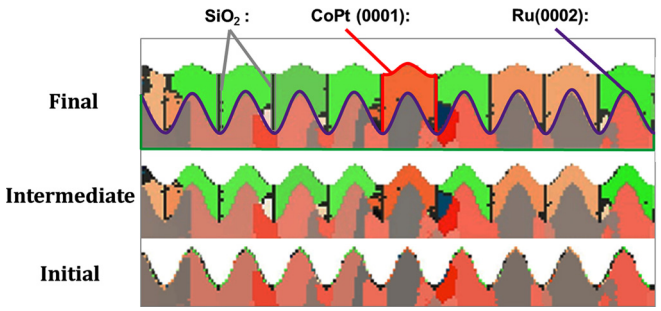

FIG. 1. Cross-sectional view of simulated CoPt (0001)+SiO_2 deposited onto the Ru (002) substrate with predefined domes. Ru is represented by grey and red colors, CoPt is represented by orange and green colors, and SiO_2 is represented by the black color.

representing the first layer being deposited. As the film grows, the film surface flattened which is similar to the experimental observations.

III. RESULTS

First, it must be mentioned that in this model, the term "T" in Eq. (3) is not the precise physical temperature of the system at which the experimental deposition process may take place. Nevertheless, in the context of simulation, the term "T" is usually referred to as the "lattice temperature." It was acknowledged[27] that lattice temperature would influence the film growth in the same way as the substrate temperature would in an experimental deposition process. Raising either the substrate temperature in the experimental deposition or the lattice temperature in the simulation would result in the introduction of thermal fluctuations into the system which leads to the occurrence of random behavior. In an experimental deposition, the thermal fluctuation causes the random walk of atoms, whereas in the MC simulation, the thermal fluctuation induces the random acceptance of certain microevents. Therefore, treating the lattice temperature "T" in the probability expression as the thermal fluctuation term allowed us to study the effect of random thermal fluctuations and obtain some qualitative insights into how the resultant film microstructure would change with the various dome ARs when a templated film growth process took place at an elevated temperature.

In a previous study,[12] it was discovered that the AR of the domes determined the magnitude of the surface energy gradient that served as the driving force for SiO_2 diffusion and hence was critical for the formation of the film microstructure. In this study, the effects of the thermal energy, in the form of "lattice temperature," on the film microstructure formation are investigated in addition to the AR of the domes. A series of templated two-phase film growth was simulated with domes of various aspect ratios (AR = 0.1–1.0) and lattice temperatures in the range of T/T_{room} = 0.1–4.0, where T_{room} is the value representing a room temperature deposition process, and the details of its determination can be found in Ref. 12. Thus, with this series of simulations, the templated growth influenced by different levels of thermal agitation, which can be interpreted as substrate temperature in the experimental sense, could be studied.

Figure 2 displays an overview of the series of simulations. The results have been divided into three regimes with respect to the lattice temperature: a kinetic limited regime, a moderate temperature regime, and a disordered regime. The diffusional behavior of the mobile species, i.e., SiO_2, according to Ref. 12 was analyzed and is shown in Fig. 3. The results will be discussed for each of these three regimes. Also, the volume fraction of the trapped SiO_2 inside the dome region, as shown in Fig. 4, was used as an indicator for the quality of the pattern in the film microstructure. The reason for such a choice was that trapped SiO_2 represents the mobile species that did not diffuse according to the global energy gradient and hence was more likely to reveal the more random behavior associated with thermal fluctuation.

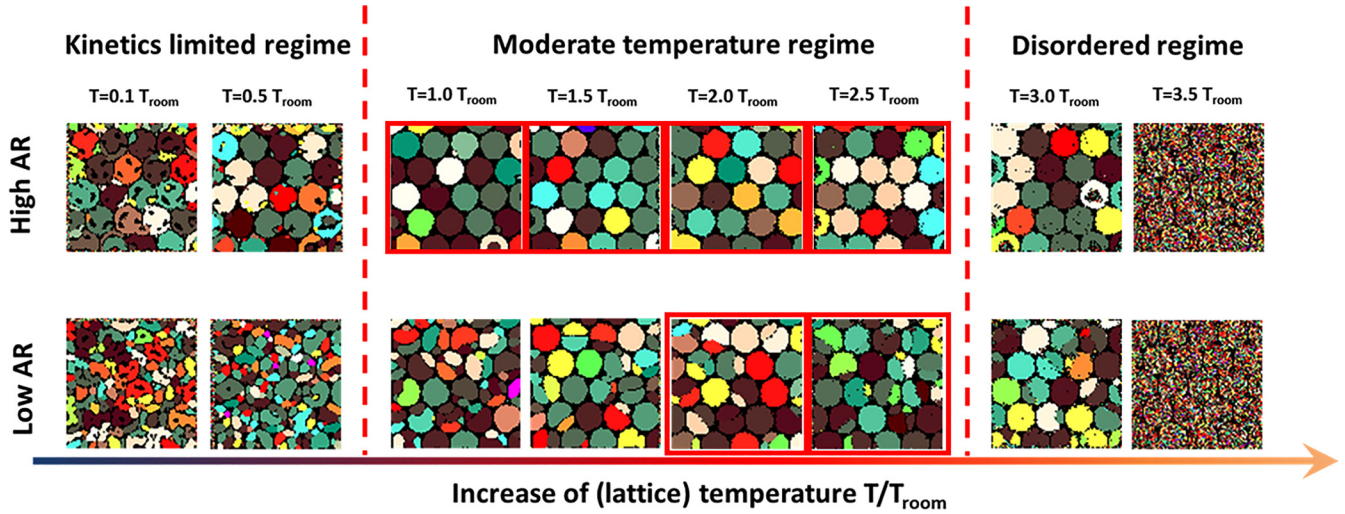

FIG. 2. Microstructure of the film deposited at different lattice temperatures k_BT ($k_BT = 0.1\ k_BT_{op}$–$4.0\ k_BT_{op}$) onto the substrate patterned with domes having different aspect ratios (ARs) (High AR = 1.0 and Low AR = 0.25). Red filled circles represent the ideal microstructure.

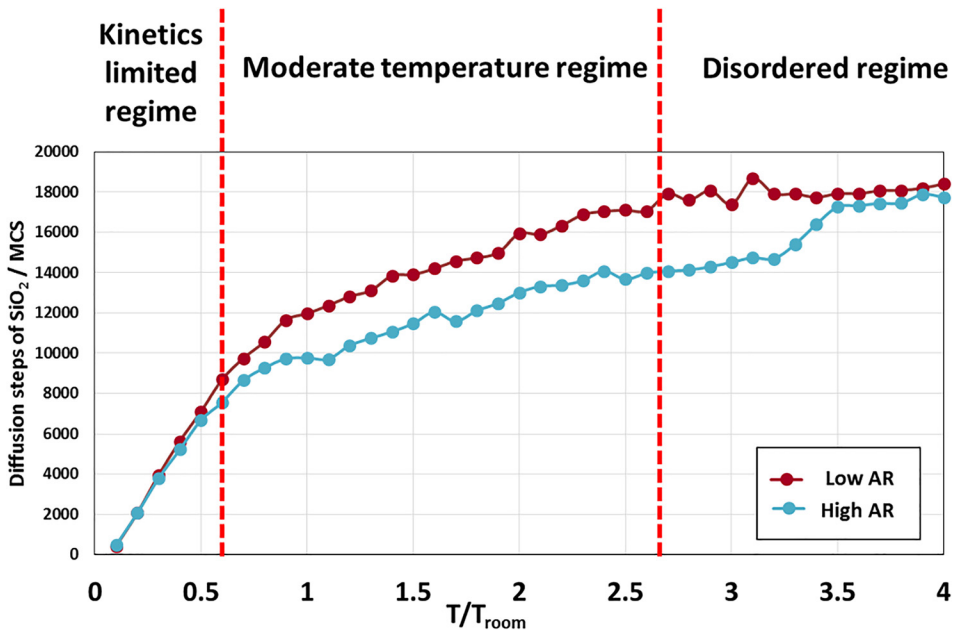

FIG. 3. Diffusion steps of SiO_2 occurred per each scanning step of systems with domes having different aspect ratios (ARs).

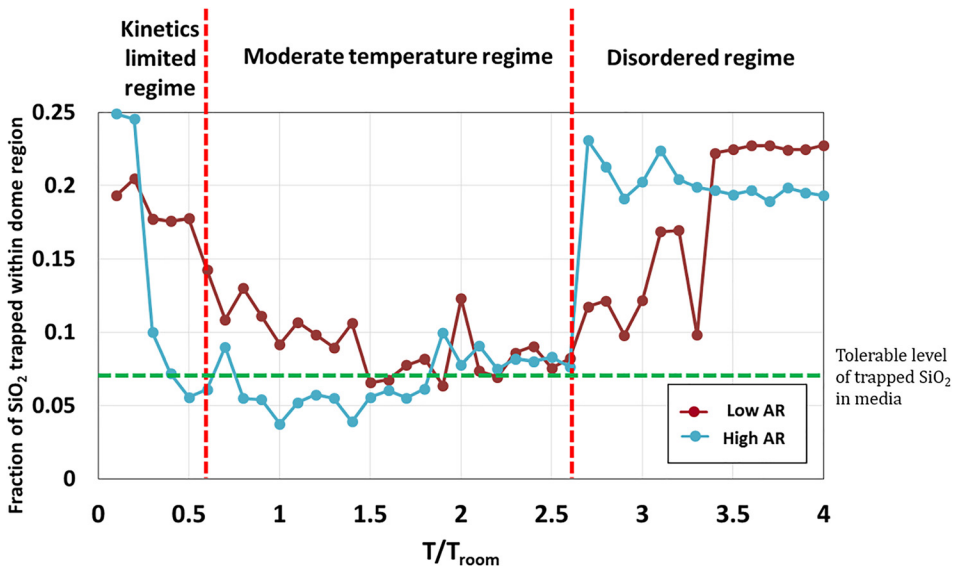

FIG. 4. SiO_2 trapped inside the dome region with domes having different aspect ratios.

The three regimes, as shown in Fig. 2, were divided according to the following considerations: (1) the characteristic microstructures, (2) the fraction of the trapped SiO_2, and (3) the overall diffusion behavior of SiO_2.

In the first regime, the characteristic microstructure was the SiO_2 clusters formed within the CoPt grains, which can be observed in Fig. 2 for both high and low AR cases. As T/T_{room} increased within this regime, the clusters of SiO_2 tend to disappear in the film grown on high AR domes, indicating a better phase separation. The temperature at which no clusters of SiO_2 formed in the high AR cases was assigned as the boundary between regime I and regime II. Such a designation was corroborated by a change in the diffusion behavior, where the total diffusion steps started to vary for high and low AR cases (shown in Fig. 3), and by a decrease in the fraction of the trapped SiO_2 shown in Fig. 4.

In the second regime, the formation of well-separated and well-ordered microstructures for high AR cases was observed. Correspondingly, the fraction of trapped SiO_2 was low, as shown in Fig. 4, in this regime. As for the low AR cases, the fraction of trapped SiO_2 was higher than high AR cases, and it should be noted that the trapping sites were mostly not inside grains but at the grain boundaries within the dome regions, which can be seen in Fig. 2. Moreover, the fraction of trapped SiO_2 for low ARs showed an interesting descending trend as the temperature increased, and it reached the same level (6–8%) in the high AR cases when T/T_{room} was beyond 2.0.

As the temperature further increased to $T/T_{room} > 2.7$, the major microstructural features observed in Fig. 2 are as follows: the random distribution of SiO_2 particles (one voxel of SiO_2) for both low and high AR cases inside CoPt grains and the appearance of a disordered structure. Thus, the third regime was called the disordered regime. The fraction of trapped SiO_2 increased continuously, up to the point that all SiO_2 became trapped SiO_2 when $T/T_{room} > 3.4$. The diffusion behavior also changed as the number of diffusion step was similar for different AR cases in Fig. 3.

The reduction of trapped SiO_2 for low ARs in the second regime was of interest since it showed a possibility of achieving an ideal patterned two-phase film using a low AR template, which is less challenging to fabricate than are the high AR templates. If the mechanisms behind such observation are understood, the fabrication process can possibly be facilitated. Therefore, in the discussion section, we will first discuss the effect of temperature on microstructure formation for moderate temperature regime in Sec. IV A. Then the results in disordered regime will be analyzed in Sec. IV B.

IV. DISCUSSION

A. In the moderate-temperature regime

In the moderate-temperature range or the second regime ($T/T_{room} = 0.7$–2.7), the ideal microstructure that follows the topography of the template was achievable under certain conditions.

With T/T_{room} being fixed at 1:1, a strong dependence between the film microstructure and AR of domes was observed. This dependency is due to the surface energy gradient introduced by the surface curvature of the topographical features, domes on our template, in accordance with Mullin's theory.[20] With a larger surface energy gradient along the dome surfaces for high ARs, this energy gradient would be sufficient to guide SiO_2 in this system to diffuse and to fill the valleys between the domes. As SiO_2 was the only material that would prevent the growth of CoPt in the system, the CoPt grain size was controlled by SiO_2. With SiO_2 segregating inside the valley as a predefined geometry on the template, the CoPt grain size and shape are controlled. Thus, less SiO_2 would be trapped inside CoPt grains, which is shown as the bluish curve in Fig. 4. This result corresponded to a low CoPt grain size distribution variance σ in Fig. 5, showing CoPt grain formation being template-controlled. If the AR was lower than the critical value of 0.6, the surface energy gradient was insufficient to fully guide the SiO_2 diffusion and desirable phase separation would not occur. In other words, the driving force by the surface energy gradient was too small to let the system overcome local energy minima, such that a fraction of SiO_2 may be trapped inside a dome region instead of filling the valleys. This is shown in Fig. 4 with trapped SiO_2 in CoPt having a value greater than the threshold trapping value. Correspondingly, the CoPt grain distribution would have a big variance σ greater than 0.3 in Fig. 5. Thus, with the AR being low, the template does not have the desired controlling effect on the film growth, while temperature was as low as $T/T_{room} = 1{:}1$.

Interestingly, as T/T_{room} was increased in the low AR cases ($AR = 0.25$) within this regime, the fraction of trapped SiO_2 continued to decrease as shown in Fig. 4. This reduction of the trapped SiO_2 indicated that the increase in temperature could potentially allow the desired microstructure formation to take place with ARs even smaller than the critical value; in other words, increasing the temperature may offer more tolerance on the AR of the template domes for the desired phase separation of CoPt and SiO_2. This is promising since a high AR of the domes is often difficult to fabricate experimentally. To obtain a rather thorough understanding of the mechanism behind these observations, the following analyses were carried out.

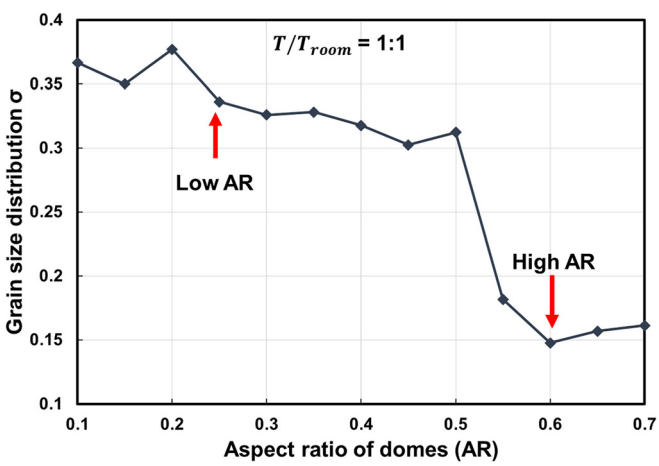

FIG. 5. Effect of the aspect ratio (AR) on the resultant grain size distribution of the thin film at fixed temperature $T/T_{room} = 1{:}1$.

First, as summarized in Fig. 3, the total number of SiO_2 diffusional attempts increased with increasing thermal energy available in the system as the lattice temperature was raised. In the MC simulations, diffusional attempts are the major means by which the system vibrates between various possible energy states, or minima, and manifests such vibration through the resultant microstructure.

Our current system includes the state of SiO_2 being trapped at the grain boundary or the state of SiO_2 filling the valleys. With more thermal fluctuations introduced into the system, the diffusional attempts became more active, allowing the system to overcome some local energy barriers and evolve toward the global energy minimum. In our system, trapped SiO_2 leaving the trapping sites inside the dome regions due to the increased number of diffusional trials is just an example of such a behavior. As more and more SiO_2 left the trapping states with increasing temperature, the grains may enlarge, predicted as zone 3 in the Structure Zone Model (SZM),[9] and hence, the grain boundaries as an energy minimum state would disappear. On the other hand, the state in which SiO_2 filled the valleys is a lower energy state than the grain boundary one. Therefore, statistically speaking, the possibility of the system finding a lower energy state becomes higher with stronger thermal fluctuations. Or, if we paraphrase this statement in terms of diffusion, then it is with stronger thermal fluctuation that the diffusion of SiO_2 would more likely to follow the direction of its geometric driving force, i.e., the surface energy gradient going from the top of the domes into the valleys.

We then investigated the interplay between the geometric driving force for the template-guided diffusion and the thermal fluctuations associated with the increasing lattice temperature. By monitoring the fraction of SiO_2 diffusion that followed the direction of the surface energy gradient, the diffusive behavior with high/low ARs at two lattice temperatures was compared. The result is shown in Fig. 6. Here, the curves were divided into segments by the cusps at almost equal intervals. Each segment represents one layer of voxels being activated for the MC runs, which simulates a layer of new materials being deposited onto the film surface. The

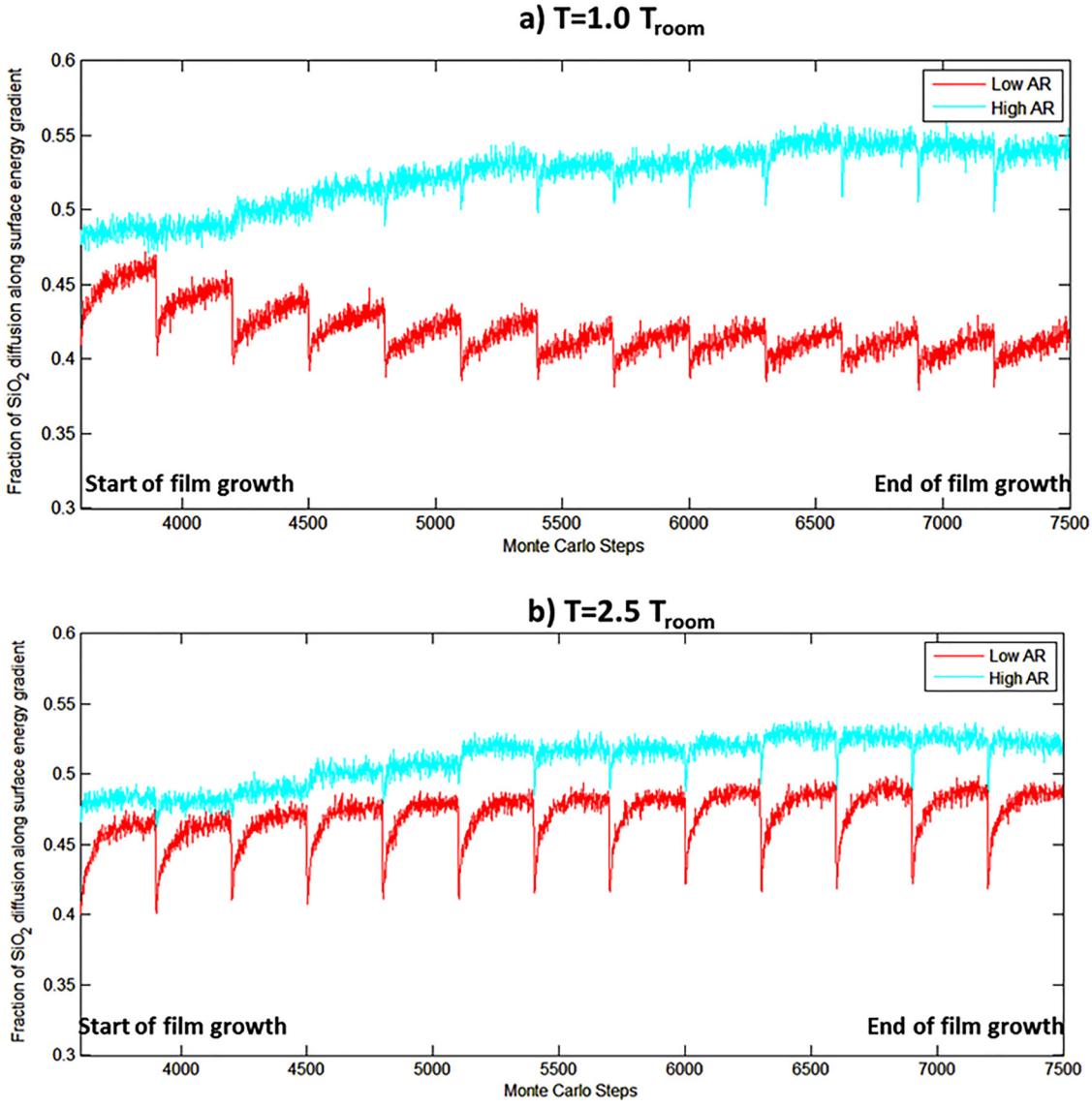

FIG. 6. Fraction of SiO_2 diffusion along the surface energy gradient (y-axis) during templated film growth with different aspect ratios (ARs) at lattice temperatures of (a) $T = 1.0\ T_{room}$ and (b) $T = 2.5\ T_{room}$.

cusps are artifacts from the scanning MC method which represents the beginning of the equilibration within each layer. In each cusp, the initial low value of the curve was due to the random state of Monte Carlo initialization. The possibility of SiO_2 diffusing along any direction was equal. As the CoPt grain grows as each layer is deposited, SiO_2 will diffuse either guided by the surface energy gradient or trapped inside the grain boundary, shown by different results in Figs. 6(a) and 6(b).

In more detail, Figs. 6(a) and 6(b) show that for the high AR cases, irrespective of the temperature, 50% of the SiO_2 diffusion occurred along the direction of the surface energy gradient, indicating it to be the dominant driving force. For the low AR cases, the guided SiO_2 diffusion increased noticeably from ~40% to ~47% when the lattice temperature increased from $T = 1.0\ T_{room}$ to $T = 2.5\ T_{room}$. This can be explained by the fact that the increase in lattice temperature induced more diffusional attempts by thermal agitation. SiO_2 could thus escape from trapping states, i.e., local minima, inside a CoPt grain on top of one dome. Therefore, it can be concluded that moderate amounts of thermal fluctuations could aid the phase separation in the simultaneous two-phase growth process even on a dome with an AR less than the critical value 0.6. In other words, the interplay between temperature and geometric features provided a possibility for developing a desirably patterned film even when the AR of the features on the template is less than ideal.

Another point to be noted is the overall number of diffusion steps of the low AR case, which was higher than that of the high AR case within the moderate temperature regime, as can be observed in Fig. 3. This was due to the stability of the system at different conditions. In the high AR case, because the surface energy gradient was greater than that in the low AR case, once SiO_2 diffused into the valley between high AR domes, it was stabilized in the valley region because it was the state with the lowest energy, unless the temperature was elevated to a much higher level that large enough thermal energy could fluctuate SiO_2 in these low energy states, as in the disordered regime. However, for low AR cases, the SiO_2 in the valley region was not as thermally stable as that in the high AR case due to the random diffusional attempts resulted from thermal fluctuation, leading to a higher overall number of diffusional steps.

B. The kinetic limited regime and the disordered regime

Regimes I and III share a common microstructural feature: a disordered mixture of the two phases, as can be seen in Fig. 2. They both have high volume fractions of trapped SiO_2 in Fig. 4. The microstructure in regime I was primarily composed of small CoPt grains in which SiO_2 clusters formed, whereas in regime III, the characteristic microstructure was patterned CoPt grains with SiO_2 randomly distributed inside the grains. As the temperature increased, in regime I, the microstructure became less disordered, while for regime III, the microstructure became more disordered. The reason why the microstructure evolved the way it did in these two regimes, even with proper driving force for diffusion present, was that the diffusion was mostly controlled by the kinetics.

During an experimental film deposition process, the frequency of atomic jumps that manifest macroscopically as diffusion increases substantially with the increasing temperature that the film is subject to. The parallel of this phenomenon in the context of MC simulations is that the acceptance of diffusion attempts increases with increasing lattice temperature. The diffusion behavior of SiO_2 in regimes I and III followed just that but with a noticeable difference, and hence, the two regimes were dubbed as a "kinetic limited regime" and a "disordered regime," respectively.

In regime I with $T/T_{room} < 0.7$, due to the lack of sufficient thermal agitation, the system was mostly "stuck" in local energy minima, unable to overcome the local energy barrier under the limited kinetics, thus forming small SiO_2 clusters reducing only the local interfacial energy. In regime III, the microstructure was partially ($2.7 < T/T_{room} < 3.4$) or fully ($T/T_{room} > 3.4$) disordered due to too strong of a thermal fluctuation at higher lattice temperature, such that the thermal fluctuation was greater than the energy barriers that stabilized the SiO_2 in the valleys and CoPt on the dome tops. As a result, the two phases in the system can no longer stay separate and became a near random mixture.

If one examines the number of diffusion steps shown in Fig. 2, it is obvious that in regime I, due to the increasing thermal fluctuations, the total number of SiO_2 diffusion steps increased and was accompanied with the disappearance of the clusters of SiO_2 within the dome regions. In regime III, apart from the same increasing trend observed in other regimes, as the lattice temperature kept increasing, after some point, the number of SiO_2 diffusion steps in Fig. 3 showed little difference for the two AR cases. This was also evident with the ~20% trapped SiO_2 shown in Fig. 4 in this high temperature regime. The thermal fluctuations dominated the film growth process, and all microevents occurred randomly, resembling a near melting state of the system when $T/T_{room} > 3.4$.

As determined with this simulation, the moderate temperature range was T/T_{room}=0.7–2.7. It was therefore reasonable to conclude that the formation of ordered microstructures during the templated two-phase film growth could be maintained at a moderately elevated temperature. If referring to the melting temperatures of CoPt and FePt, (i.e., 1763 and 1873 K, respectively), and making them the lattice temperature at which the complete disordered microstructure appeared as the melting temperature, we can estimate $T_{melt}/T_{room} \sim 3.4$, which gave the moderate temperature range roughly 1000 K. This is a very rough estimate, and the temperature range could be better estimated with an *ab initio* computation. Nevertheless, this does provide some insight into the fabrication process of CoPt and FePt based composite magnetic recording media.

V. CONCLUSION AND FUTURE WORK

1. The resultant film microstructures during templated growth at different lattice temperatures and with domes of different aspect ratios were studied. Three regimes were

determined with regard to both the microstructure and the diffusion behavior of the mobile species.
2. With the necessary driving force for surface diffusion present, the thermal fluctuations introduced into the system with increasing lattice temperature were shown to be essential for the phase separation to take place and hence the formation of the desired microstructure, as in regime II. The lack of sufficient thermal fluctuations resulted in clustering of SiO_2 (regime I), whereas too much of it resulted in destabilized phase separation and a disordered microstructure (regime III).
3. An elevated lattice temperature was also shown to increase the tolerance of the aspect ratio of the dome for obtaining desired film microstructures within a moderate temperature range, such that an aspect ratio lower than a previously determined critical value may suffice a successful templated growth.
4. The concentration of SiO_2 was set 25% throughout this simulation. In the vicinity of the 25% concentration, addition of SiO_2 would be expected to limit the CoPt grain growth, while depletion of SiO_2 would lead to incomplete SiO_2 coverage on grain boundaries. Both will worsen the magnetic property of the thin film. However, when temperature and template were also changed, no accurate prediction could be made beyond this point. Thus, the effect of the SiO_2 concentration in the presence of other parameters remains to be studied for the CoPt+ SiO_2 system.

ACKNOWLEDGMENTS

The authors acknowledge the use of the Parallel Grain Growth programs developed in the Department of Materials Science and Engineering at Carnegie Mellon University. Also, the National Science Foundation of China, Guangdong Province, project fund (No: 2015A030310281) is acknowledged. The authors would like to thank Vignesh Sundar, a former graduate student of the Department of Materials Science and Engineering at Carnegie Mellon University, for the help in the programs.

APPENDIX: DETERMINATION OF ENERGETIC TERMS

In order to best represent the physical behavior of each component material during deposition as described in Ref. 1, the magnitude of energetic terms that dominantly affect the diffusive behavior, i.e., $\gamma_{seg/MM}$, γ_{GB}, and $\gamma_{MM/sub}$, was carefully determined by the following steps:

First, in order to simulate the simplest scenario, i.e., experimental deposition on a flat substrate[1] with CoPt grains being partially (~70%) occupied, a series of Monte Carlo simulations was conducted with only γ_{GB} and $\gamma_{seg/MM}$ being effective: initially, CoPt voxels having different in-plane orientations and SiO_2 voxels are randomly distributed in a simulation box in which periodic boundary conditions were applied along x-y dimensions; the ratio $\gamma_{GB}/\gamma_{seg/MM}$ was varied in a wide range from 0.4:1 to 5:1 to inspect that after the Monte Carlo equilibration process, whether SiO_2 can segregate into GB and partially cover the CoPt grains as observed experimentally. In Fig. 7, the percentage of GB being covered was denoted as η_{GB} which was used as a metric for model evaluation.

When this ratio is too low, i.e., less than 1:1, the SiO_2/CoPt interface is less favored. Formation of SiO_2 clusters is observed in Fig. 7 (1), in which the SiO_2/CoPt interfacial area is minimized, as the black particles (SiO_2) coexisting with CoPt grains (represented by other colors). However, when this ratio is too high, CoPt grains are completely covered by SiO_2, shown as case (3). This complete grain boundary segregation does not occur in the CoPt-SiO_2 system, and thus, high $\gamma_{GB}/\gamma_{seg/MM}$ is not considered in our model. It is interesting to note that there is a strong dependency between GB segregation and the interfacial energy ratio. A potential interpretation is that whichever interface that has the lower energy will be preferred, with two extremes shown in the cases (1) and (3), in which the former favored GB and the latter favored the SiO_2/CoPt interface. Therefore, an intermediate ratio $\gamma_{GB}/\gamma_{seg/MM} = 2.2{:}1$ is chosen in our model as the optimal ratio, which is shown by case (2) in Fig. 7 with $\eta_{GB} \sim 70\%$ GB that matches the experimental result in Ref. 1 well.

Second, the epitaxial interface between the substrate Ru and the deposited CoPt is set to have the lowest interfacial energies. A relative ratio $\gamma_{MM/sub} : \gamma_{seg/MM} : \gamma_{GB} = 1 : 5 : 11$ with respect to other terms is established. Taking $\gamma_{MM/sub} = 0.1\ \mathrm{J}/m^2$ and $\gamma_{GB} = 1.1\ \mathrm{J}/m^2$, an approximation of the epitaxial CoPt/Ru interface and typical grain boundaries with a small misorientation can be represented. $\gamma_{seg/MM} = 0.5\ \mathrm{J}/m^2$ is determined by the parametric search.

The remaining surface energy terms, i.e., E^{S}_{CoPt} and $E^{s}_{SiO_2}$, are determined by a similar parametric search strategy. The broken-bond theory[28] is utilized, which treats the bond strength equivalent to the surface energy divided by the number of bonds in unit area. Thus, the influence of surface energy terms is determined as follows:

Consider the mobility of each species in Eq. (3) using the Boltzmann expression: $M = M_0 \times \exp(-E^{Act}/kT)$. The activation E^{Act} is treated as the equivalent to the energy increase by breaking the bonds during the transition state of possible Monte Carlo swap of materials. SiO_2–SiO_2 bond

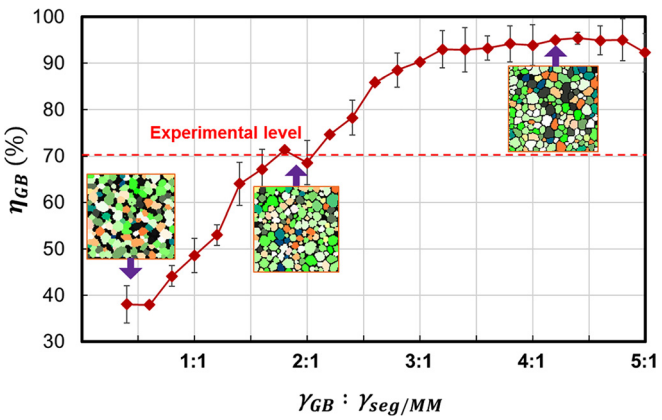

FIG. 7. Influence of interfacial energy on the two-phase film grown on a flat substrate with respect to GB coverage by SiO_2 in percentage. The corresponding microstructure is presented by a plane view as the insets: black represents SiO_2, and other colors represent CoPt grains in different in-plane orientations.

strength could thus be derived from SiO_2 surface energy, which is 1.5 J/m^2 according to Ref. 25. The CoPt–SiO_2 "bond" can be determined by $E^{S}_{CoPt} + E^{s}_{SiO_2} - \gamma_{seg/MM}$, with E^{S}_{CoPt} being undetermined. E^{S}_{CoPt} would vary based on different facets according to Ref. 24. An energy sweeping process was conducted with known $E^{s}_{SiO_2}$ and $\gamma_{seg/MM}$. It was found that, with E^{S}_{CoPt} being too low, CoPt-CoPt bonds are unrealistically weak, leading to surface segregation of CoPt, which contradicts experimentally observed surface coverage of SiO_2. With E^{S}_{CoPt} being too high, SiO_2 becomes extraordinarily diffusive. The highly mobile SiO_2 results in a dispersive distribution of SiO_2 throughout the film. This mixing of SiO_2 and CoPt is contrary to the fact that SiO_2 and CoPt are immiscible materials. Hence, a value of $E^{S}_{CoPt} = 2.1\,J/m^2$ is selected which preserves the partial segregation of SiO_2 into the CoPt grain boundary. This value is also reasonable compared to the computation result in Ref. 24.

The final ratio between all energy terms can thus be established as follows: $\gamma_{MM/sub} : \gamma_{GB} : \gamma_{seg/MM} : E^{s}_{SiO_2} : E^{s}_{CoPt} = 1 : 5 : 11 : 15 : 21$. The room temperature term is used as $\gamma_{MM/sub} : kT = 1.2 : 1$ to simulate the room temperature deposition result in experiment. The detailed study of the temperature effect is included in the main text.

[1]V. Sundar, J. Zhu, D. E. Laughlin, and J.-G. Zhu, "Novel scheme for producing nanoscale uniform grains based on templated two-phase growth," Nano Lett. **14**(3), 1609–1613 (2014).

[2]E. Yang *et al.*, "Templated-assisted direct growth of 1 Td/in^2 bit patterned media," Nano Lett. **16**(7), 4726–4730 (2016).

[3]C. Park, J. Yoon, and E. L. Thomas, "Enabling nanotechnology with self assembled block copolymer patterns," Polymer **44**, 6725–6760 (2003).

[4]S. K. Sivaraman and V. Santhanam, "Realization of thermally durable close-packed 2D gold nanoparticle arrays using self-assembly and plasma etching," NanoTechnology **23**, 255603 (2012).

[5]B. D. Terris and T. Thomson, "Nanofabricated and self-assembled magnetic structures as data storage media," J. Phys. D: Apply. Phys. **38**, R199 (2005).

[6]J. C. Mallinson, "A new theory of recording media noise," IEEE Trans. Magn. **27**(4), 3519–3531 (1991).

[7]V. Sokalski, D. E. Laughlin, and J.-G. Zhu, "Experimental modeling of intergranular exchange coupling for perpendicular thin film media," Appl. Phys. Lett. **95**, 102507 (2009).

[8]H. Wang *et al.*, "Fabrication of FePt type exchange coupled composite bit patterned media by block copolymer lithography," J. Appl. Phys. **109**, 07B754 (2011).

[9]J. A. Thornton, "High rate thick film growth," Ann. Rev. Mater. Sci. **7**(1), 239–260 (1977).

[10]P. B. Barna and M. Adamik, "Fundamental structure forming phenomena of polycrystalline films and the structure zone models," Thin Solid Films **317**, 27 (1998).

[11]A. Anders, "A structure zone diagram including plasma-based deposition and ion etching," Thin Solid Films **518**, 4087–4090 (2010).

[12]X. Lu, B. Lai, V. Sundar, J.-G. Zhu, D. Laughlin, and J. Zhu, "Understanding the nanostructure formation of the templated two-phase film growth via hybrid modeling," Cryst. Growth Des. **17**(3) 1016–1027 (2017).

[13]V. Sundar, "Templated two-phase growth of magnetic recording media," Ph.D. thesis (Carnegie Mellon University, Pittsburgh, 2014).

[14]J. A. Sethian, *Level Set Methods and Fast March Methods Evolving Interfaces in Computer Geometry, Fluid Mechanics, Computer Vision, and Material Science* (Cambridge University Press, New York, 2005), p. 1.

[15]S. Osher and R. P. Fedkiw, "Level set methods: An overview and some recent results," J. Comput. Phys. **169**(2), 463–502 (2001).

[16]R. B. Potts, Math. Proc. Cambridge Philos. Soc. **48**(1), 106 (2008).

[17]A. J. Francis *et al.*, "Monte Carlo simulations and experimental observations of templated grain growth in thin platinum films," Acta Mater. **55**, 6159–6169 (2007).

[18]Y. G. Zheng *et al.*, "Monte Carlo simulation of grain growth in two-phase nanocrystalline materials," Appl. Phys. Lett **88**, 144103 (2006).

[19]E. A. Holm, D. J. Srolovitz, and J. W. Cahn, "Microstructural evolution in two-dimensional two-phase polycrystals," Acta Metall. Mater. **41**(4), 1119–1136 (1993).

[20]W. W. Mullins, "Mass transport at interface in single component systems," Metall. Mater. Trans. A **26**(8), 1917–1929 (1995).

[21]A. Dannenberg, M. E. Gruner, A. Hucht, and P. Entel, "Surface energies of stoichiometric FePt and CoPt alloys and their implications for nanoparticle morphologies," Phys. Rev. B **80**(24), 245438 (2009).

[22]A. F. Voter and J. D. Doll, "Transition state theory description of surface self-diffusion: Comparison with classical trajectory results," J. Chem. Phys. **80**, 5832 (1984).

[23]D. G. Truhlar and B. C. Garrett, "Current status of transition-state theory," J. Phys. Chem. **100**, 12771 (1996).

[24]A. Pascal, P. B. Véronique, T. Florent, A. V. Caroline, and D. Véronique, "Structure and order in cobalt/platinum-type nanoalloys: From thin films to supported clusters," Surf. Sci. Rep. **70**, 188 (2015).

[25]Y. K. Shchipalov, "Surface energy of crystalline and vitreous silica," Glass Ceram. **57**(11-12), 374 (2000).

[26]J. W. Evans, P. A. Thiel, and M. C. Bartelt, "Morphological evolution during epitaxial thin film growth: Formation of 2D islands and 3D mounds," Surf. Sci. Rep. **61**(1-2), 1–128 (2006).

[27]D. Zöllner, "A new point of view to determine the simulation temperature for the Potts model simulation of grain growth," Comp. Mat. Sci **86**, 99–107 (2014).

[28]M. Hanoch *et al.* "Models for adatom diffusion on fcc (001) metal surfaces," Phys. Rev. B **60**(3), 2106 (1999).